Supplemental Figure 1 (Related to Figure 1)

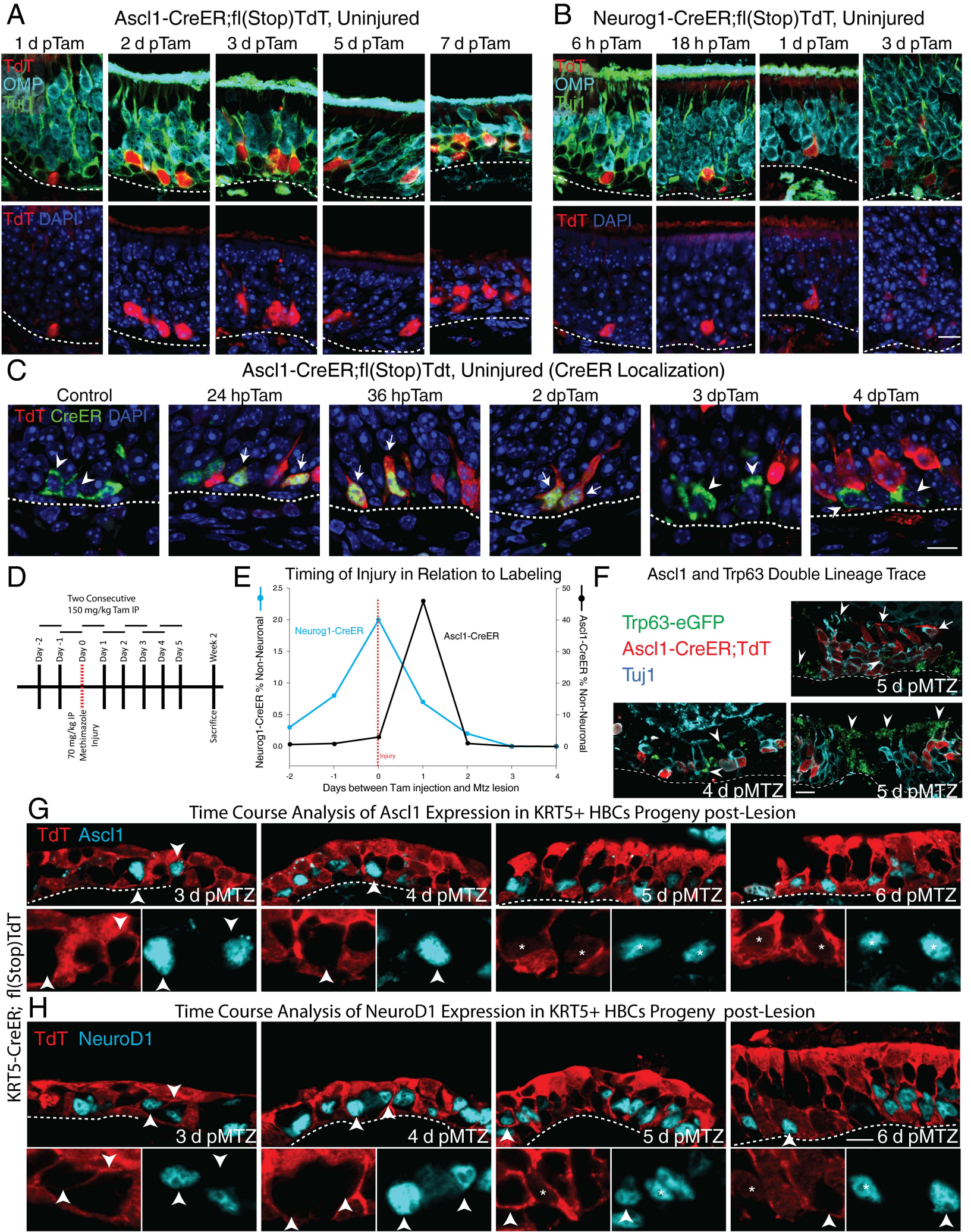

Supplemental Figure 2 (Related to Figure 2)

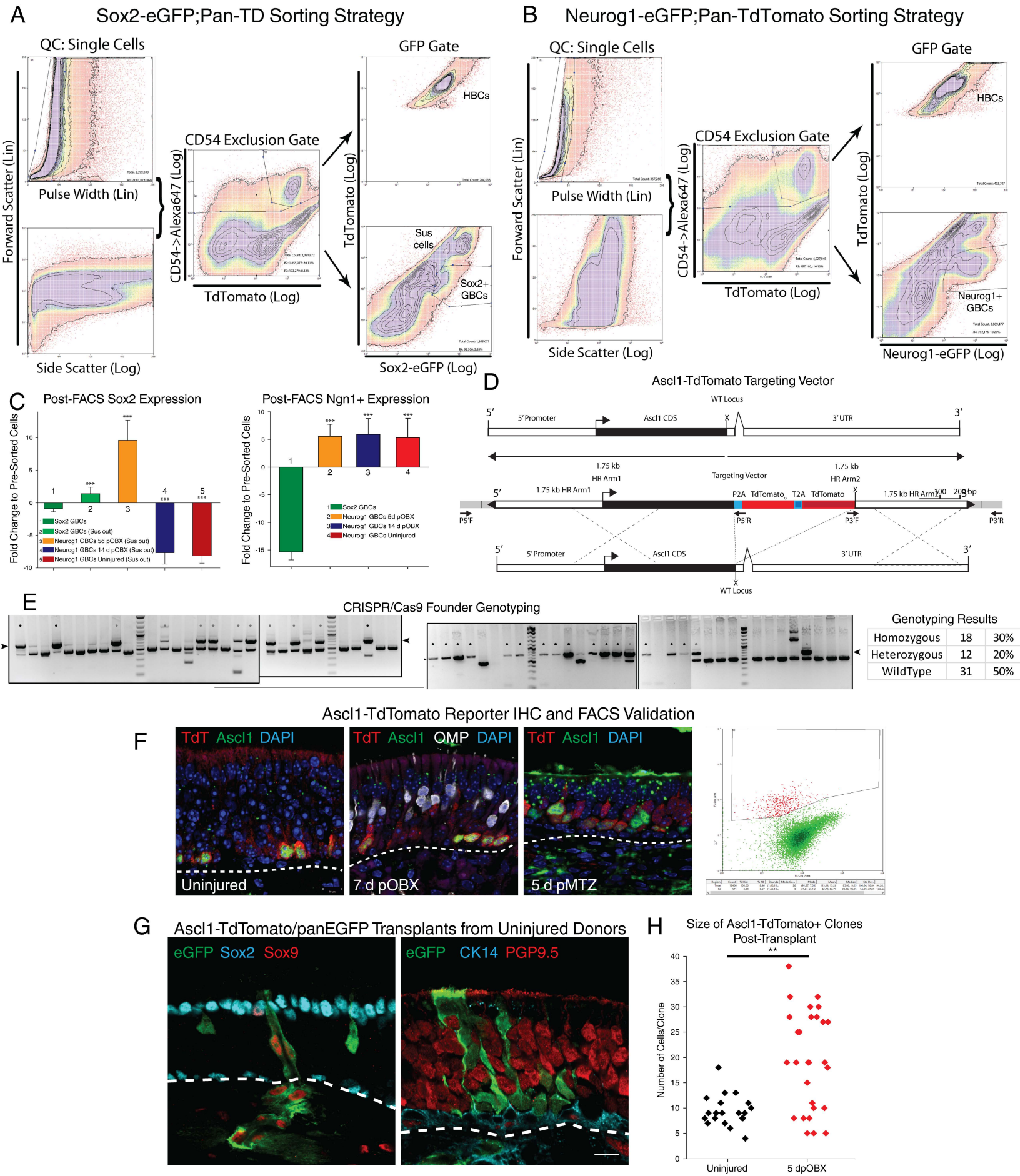

Supplemental Figure 3 (Related to Figure 3)

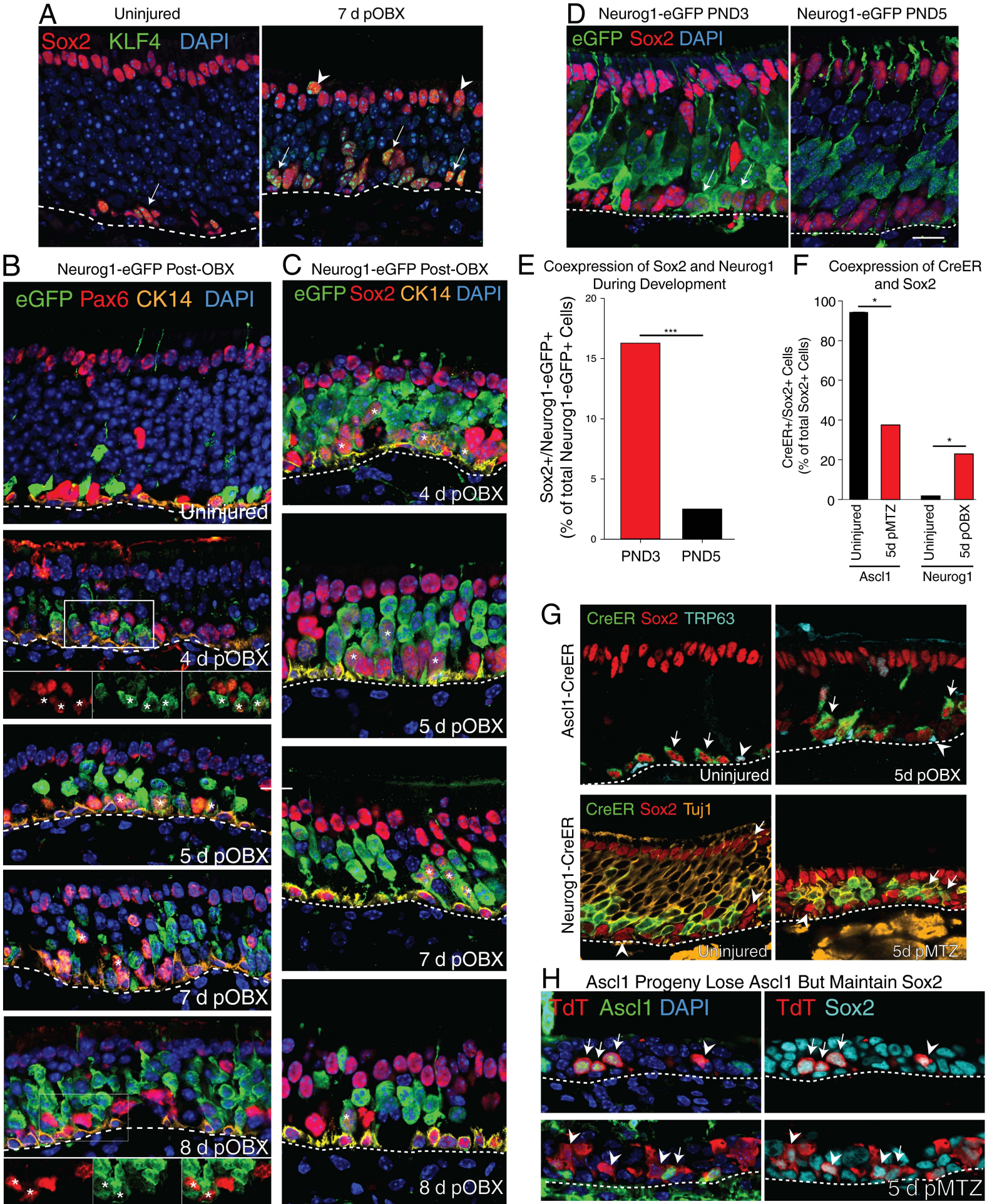

Supplemental Figure 4 (Related to Figure 4)

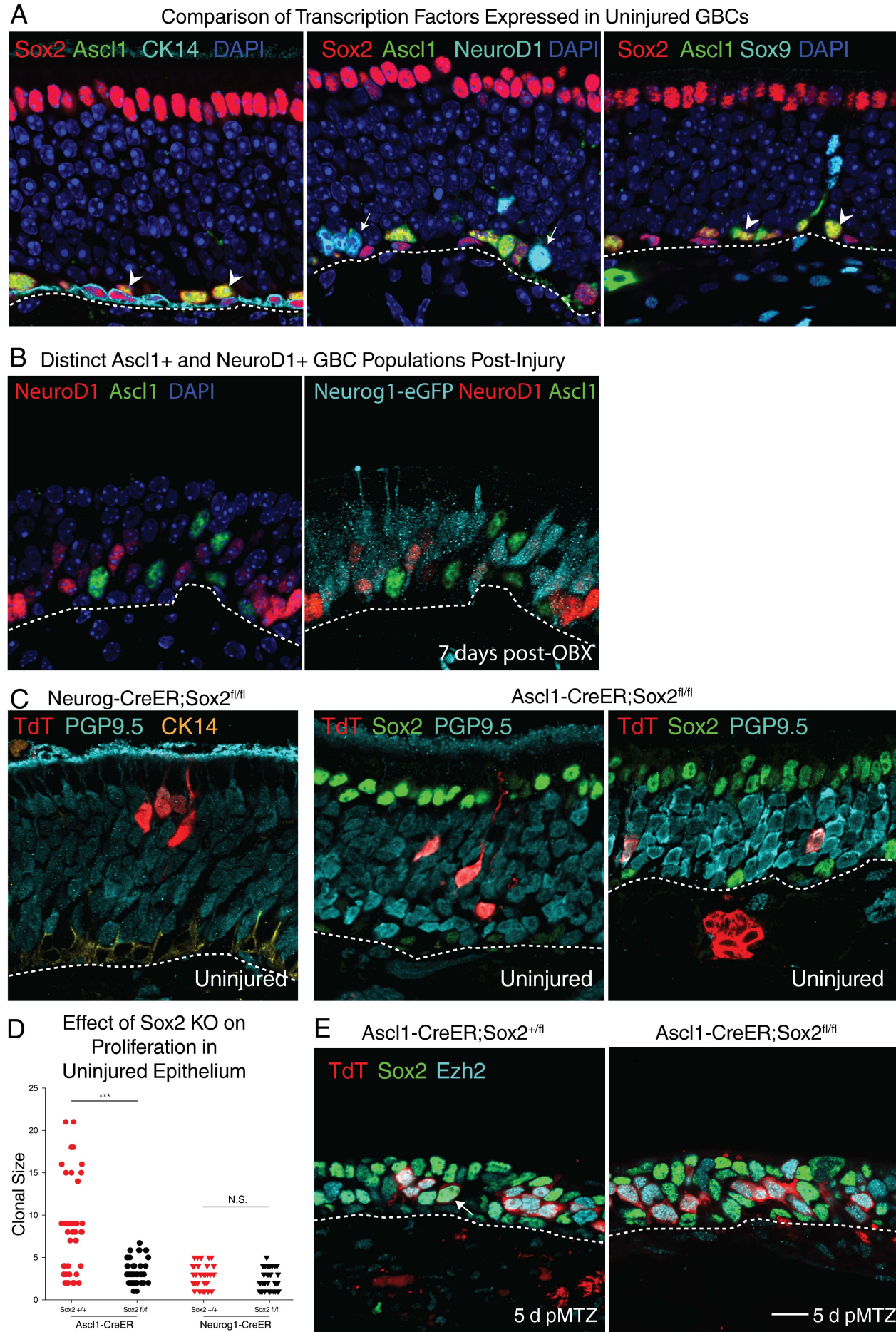

Supplemental Figure 3 (Related to Figure 3)

A

Single Cell QC Statistics

Single Cells Captured	140
Post-QC Filter	120
Average Reads/Cell	2419706
Mean Quality Score	36.1944
%≥ Q30 bases	92.66539
Average Unique Mapped Read Pairs	1,889,995
Average Mapped Percentage	62.63%
Average RefSeq Transcripts Detected	15,472
Post Filter Genes Detected	10,579

B

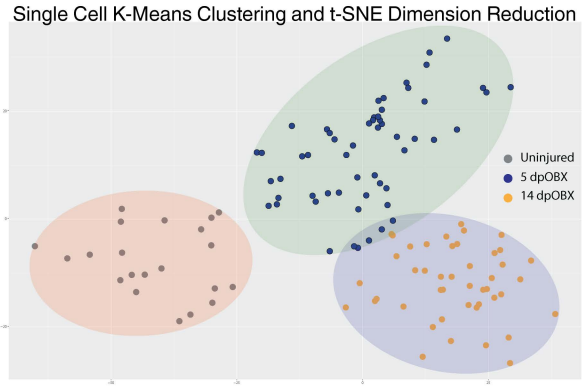

C

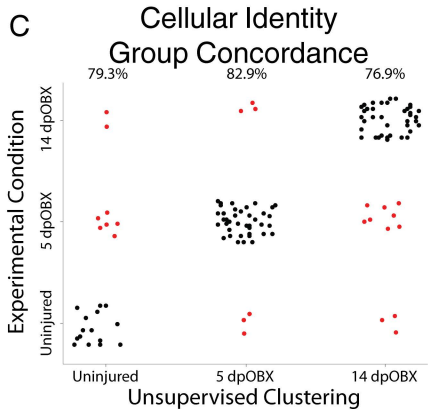

D

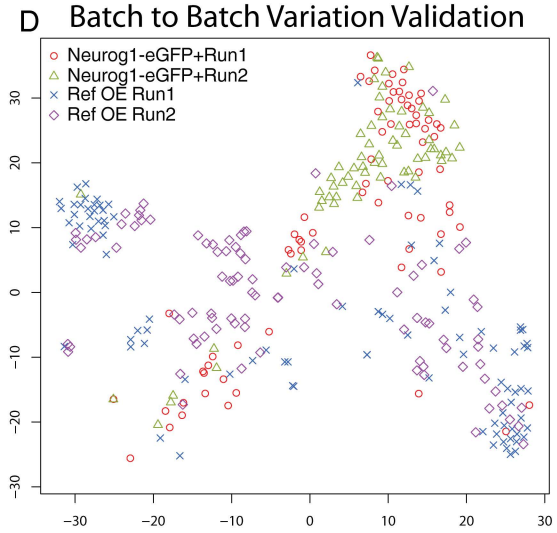

E

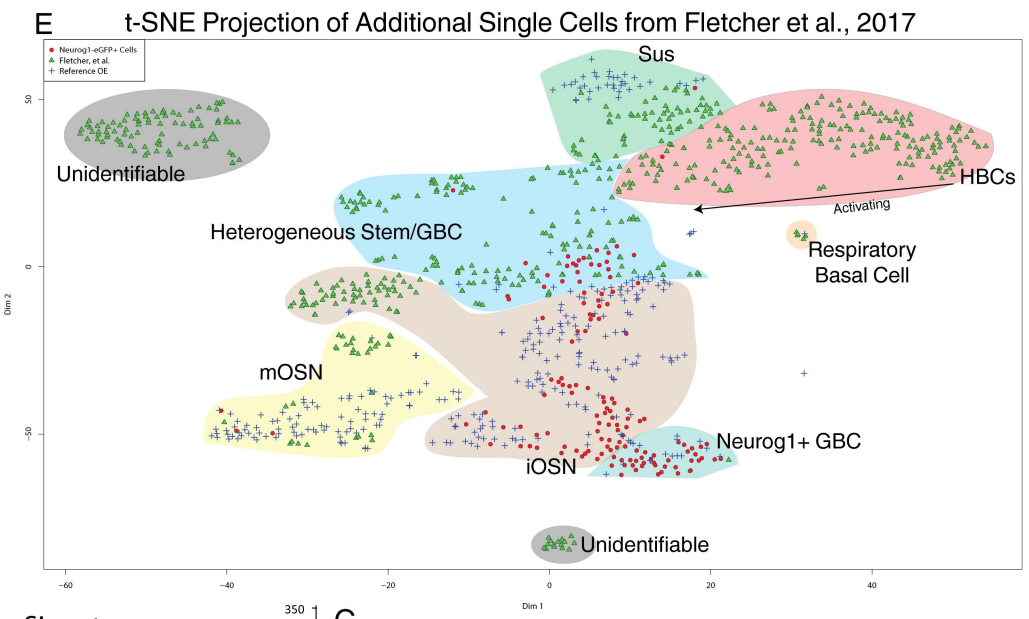

F

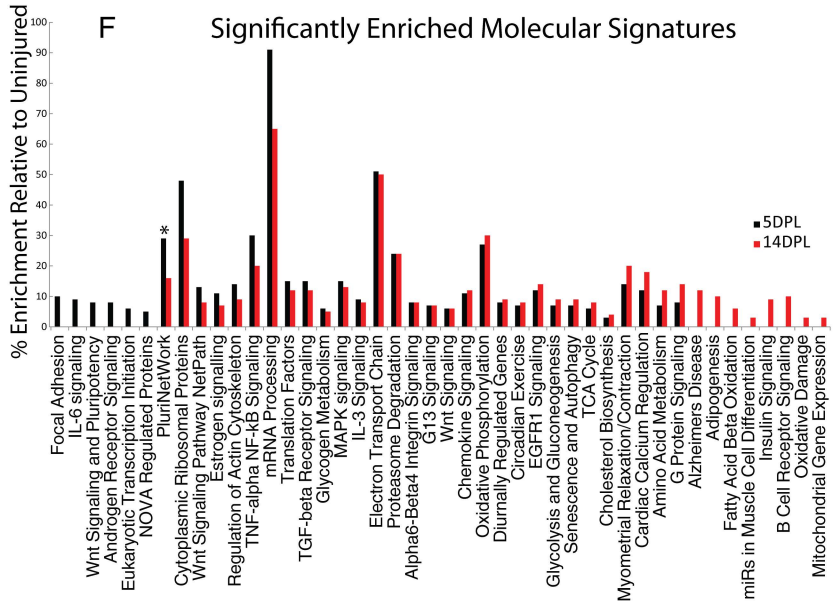

G

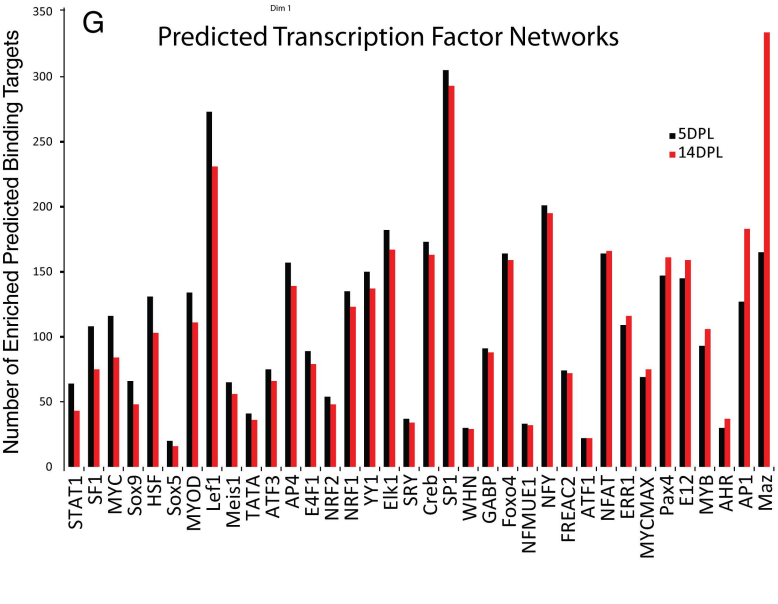

H

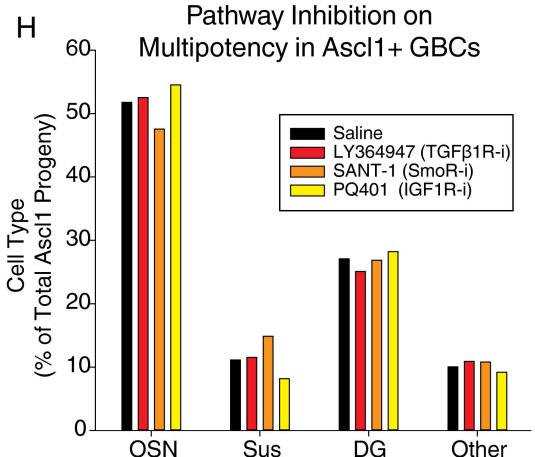

I

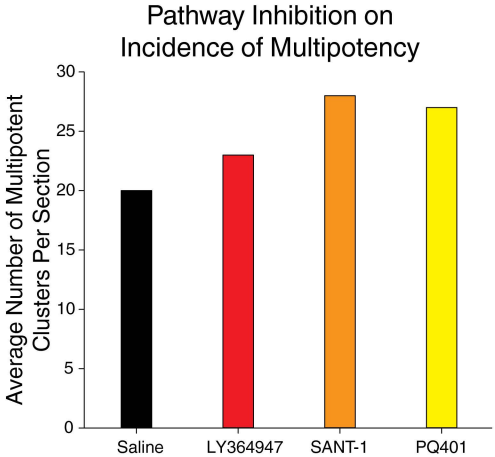

Figure S1 Related to Figure 1

(A, B) In uninjured epithelium, both Ascl1+ and Neurog1+ progenitors promote quickly from the GBC compartment and differentiate into neurons as shown by pulse-chase experiments using Ascl1 or Neurog1-CreER drivers and IHC staining for TdT (red), OMP (cyan), and Tuj1 (green) as a function of time after recombination. Tamoxifen injected IP at 150 mg/kg for two consecutive days. The scale bar in B equals 10 µm and applies to A and B. (C) Tamoxifen injected IP at 150 mg/kg for two consecutive days induces nuclear localization of CreER (driven by Ascl1-CreER) and TdT induction, which ceases by 3 days after the second injection. The arrowheads indicate cells in which CreER is cytoplasmic, while the arrows indicate cells in which CreER is nuclear. The scale bar equals 10 µm. (D) Graphic depiction of Tam and methimazole (MTZ) dosing strategy to determine the window between Tam injection and lesion that labels the maximal number of multipotent progenitors. (E) Percentages of non-neuronal cells generated *in situ* in the Neurog1 and Ascl1-CreER lineages as a function of the interval between Tamoxifen doses and epithelial injury using the paradigm shown in C. Promotion to multipotency occurs over a very narrow window relative to the timing of the lesion, catching the progenitors before they progress to terminal differentiation. (F) Double lineage trace using Ascl1-CreER;fl(Stop)TdTomato and Trp63-eGFP, 4 and 5 days post-MTZ injury. The multiple panels at 5 days post-MTZ injury demarcate the observed extent of eGFP staining variability. The arrowheads mark eGFP+ only cells, while the arrows mark TdTomato+ only cells. The scale bar equals 10 µm. (G-H) Post-MTZ interval at which either (F) Ascl1+ or (G) NeuroD1+ GBCs is detected by IHC relative to the timing of their differentiation from activated HBCs as marked by KRT5-CreER lineage tracing prior to lesion. Neither type of GBC emerges from HBCs during the interval when Tamoxifen-induced recombination takes place in the GBCs. The arrowheads indicate Ascl1+ or NeuroD1+ only cells, while the asterisks mark Ascl1 or NeuroD1/TdTomato double-positive cells. As cytoplasm is particularly limited in these cells, note the faint, nuclear TdT found in the asterisk-marked cells that is absent from the arrowhead-marked, non-TdT positive cells. The scale bar in H equals 10 µm and applies to G and H.

Figure S2 Related to Figure 2

(A, B) FACS strategy for isolating either Sox2-eGFP;pan-TD cells (A) or Neurog1-eGFP;pan-TD cells (B). Single cell gating on forward scatter and side scatter is followed by removal of HBCs using a CD54-exclusion gate (Top), and finally gating for eGFP-mid-intensity cells (Bottom). (C) qRT-PCR of FACS-isolated cells assessing enrichment of Sox2 or Neurog1 mRNA. RNA levels were compared to whole dissociated OE cells pre-sort. Where marked as “Sus out,” inputs were first Sus cell depleted prior to

qRT-PCR to reflect more appropriate Sox2 enrichment levels. (D) Graphical schematic of the targeting construct used for CRISPR-Cas9-mediated homologous recombination and generation of the Ascl1-TdTomato^{2} mouse. The knock-in location is immediately downstream of the Ascl1 coding sequence and the targeting vector is fused to two concatenated TdTomato sequences separated by 2A peptide sequences. Genotyping primers used to confirm successful knock-in are marked on the targeting vector. (E) DNA agarose gel showing genotyping results of the first generation founders. The red arrow indicates the mutant band. Red dots mark homozygous knock-in mice, while green dots mark heterozygous ones. The table summarizes the CRISPR knock-in efficiency. (F) IHC confirmation that bright TdTomato labeling co-localizes with Ascl1 protein, whether in OE from uninjured mice or post-injury (7 d pOBX or 5 d pMTZ); faint TdTomato labeling is found in immature neurons due to TdTomato perdurance. Scarcity of OMP (white) confirms successful bulbectomy. The scale bar equals 10 µm. The FACS plot shows successful separation of brightly-labeled TdTomato+ cells. (G) IHC of clones that were generated by Ascl1+ cells isolated from uninjured donors transplanted into a lesioned host animal by intranasal infusion, showing PGP+ neurons, Sox9+ D/G cells, apically located Sus cells, and CK14-/PGP- GBCs. The scale bar equals 10 µm. (H) Analysis of clone size demonstrates that Ascl1-TdTomato+ cells harvested 5 day post-OBX generate larger clones than cells from uninjured animals. ** $p<0.001$ Mann-Whitney Rank Sum.

Figure S3 Related to Figure 3

(A) IHC staining demonstrating expanded numbers of cells positive for KLF4 and Sox2 7 days after bulbectomy as compared to uninjured tissue; the arrowheads mark apical cells expressing KLF4, while the arrows mark the basal ones. (B) IHC staining for Pax6 as function of time after bulbectomy (pOBX) demonstrating the induction of Pax6 expression in Neurog1+ GBCs. The asterisks mark double-labeled cells in the split channel insets. (C) IHC staining for Sox2 as function of time after bulbectomy using a different rat anti-Sox2 antibody, which confirms and validates the specificity of the staining in Figure 4C. The asterisks mark double-labeled cells. (D) IHC staining for Sox2 and Neurog1-eGFP in the OE at post-natal days 3 and 5; the arrows mark Neurog1-eGFP/Sox2 double-positive cells. The scalebar equals 10 µm and applies to all panels (except insets). (E) Counts of Sox2/Neurog1-eGFP double-positive cells at the postnatal time points illustrated in (D) (n=3); *** $p < 0.001$ Mann-Whitney Rank Sum. (F) Counts of either Ascl1-CreER+/Sox2+ or Neurog1-CreER+/Sox2+ double positive cells in either uninjured or injured tissue. (n=3); * $p>0.01$ Mann-Whitney Rank Sum. (G) IHC staining of samples of the tissue counted in (F). Arrows mark CreER+/Sox2+ double-positive cells. The arrowheads in the top panel depict HBCs that

were excluded from the counts as identified by TRP63 staining. The arrowheads in the bottom panel depict single Sox2+ cells that are not CreER+. (H) IHC staining of Ascl1-CreER-derived cells at 5 days post-MTZ injury demonstrating the loss of Ascl1 (green) in the lineage-traced cells (red) that retain Sox2 (cyan) expression; Tam was administered as previously for Ascl1-CreER lineage tracing. The arrows mark triple-positive cells demonstrating efficacy of staining, while the arrowheads mark lineage-traced cells that are Ascl1(-) but Sox2(+). The two panels demonstrate the extent of variability observed in the tissue, where some regions are dominated by non-dedifferentiating cells (top) while others contain mostly Ascl1(+), Sox2(+) dedifferentiating cells.

Figure S4 Related to Figure 4

(A) IHC staining for transcription factors Sox2, Ascl1, NeuroD1, and Sox9 in uninjured OE tissue. Ascl1+ GBCs express Sox2, while NeuroD1+ GBCs do not. Ascl1+ GBCs do not co-express Sox9, a marker of differentiated duct/gland cells. The arrowheads indicate double-labeled, Sox2+ and Ascl1+ GBCs, the arrows indicate single-labeled NeuroD1+ GBCs. (B) IHC staining for Ascl1, NeuroD1, and Neurog1-eGFP demonstrating that Ascl1+ and NeuroD1+ cells are distinct populations. (C) IHC staining of clones generated *in situ* from Neurog1-CreER- or Ascl1-CreER-driven Sox2 knockouts. (D) Size of clones generated *in situ*, comparing heterozygous vs. homozygous floxed Sox2 mice using Neurog1 or Ascl1-CreER drivers in uninjured OE. (E) IHC for Sox2 and Ezh2 shows that they are reciprocal in labeling in the OE from heterozygous and homozygous floxed Sox2 mice 5 days post-MTZ. Ezh2+ cells are more numerous in the homozygous mice. The scale bar equals 10 μm and applies to all panels (except insets).

Figure S5 Related to Figure 5

Analysis of single cell RNAseq transcriptomes. (A) Quality control statistics of single cell capture and RNAseq filtering. (B) t-distribution Stochastic Neighbor Embedding (t-SNE) dimension reduction of Neurog1-eGFP+ cells isolated from uninjured, 5 and 14 dpOBX. Three clusters were assigned without a priori knowledge of cell identity and cells were identified post hoc as to group. (C) Two captures, each containing two experimental conditions were performed. TdTomato marker was used to delineate between each condition within a run, with the 5 d OBX-tissue being duplicated to allow for tiling normalization for batch effects. Here, a matrix shows the concordance between conditions determined using TdTomato marker (marked as Experimental Condition) and group identity determined de novo as shown in Figure S5B. Some discordance is expected, due to noise in detecting the TdTomato label, as well as natural variance in cell identity when bioinformatically

determining group identity. (D) t-SNE plot overlaid with batch run identities, demonstrating significant batch-to-batch overlap and ruling out batch-related effects. (E) t-SNE plot combining the dataset collected in this study (red dots and blue crosses) and a recently published dataset (Fletcher et al., 2017) of quiescent HBCs and their progeny after forced activation by artificial TRP63 knockout (green triangles). Activated HBCs generate GBCs, labeled in blue shading, which are able to form multiple cell types; the HBC-derived GBCs mesh with Neurog1-eGFP+ GBCs post-injury. Lack of mixing can be attributed to differences in experimental conditions and isolation procedures. (F) Bar graph of significantly enriched molecular signatures at 5 days post-bulbectomy (DPL) and 14 days DPL as compared to uninjured as determined by WebGestalt operating on Broad Institute Gene Signatures. (G) Bar graph of transcription factor networks that had significant enrichment of downstream targets under the same post-injury conditions. (H) Quantitative assessment of cell types generated by Ascl1-CreER+ GBCs *in situ* following intranasal infusion of inhibitors of signaling pathways including saline vehicle, LY364947 (TGFβR inhibitor), SANT-1 (Hedgehog/Smo inhibitor), and PQ401 (IGF-1R inhibitor) (n=3); * $p < 0.05$, Kruskal-Wallis ANOVA on Ranks. Counts are depicted as a percentage of total counted cells, pooled across replicate conditions. (I) Counts of the number of clusters containing multiple cell types per section, pooled across replicate conditions, as a proxy for measuring efficiency of multipotency induction (n=3); * $p < 0.05$, Kruskal-Wallis ANOVA on Ranks.

Table S1. Antibodies used for Immunohistochemistry Table, Related to STAR Methods

Primary Antibody	Protocol	Cell Type(s) marked
RbαCK14	1:400 2°	HBCs
GtαCK14	1:50 2°	HBCs
RbαmCherry	1:100 2°	TdTomato+
GtαmCherry	1:150 2°	TdTomato+
RbαPGP9.5/UCHl1	1:300 2°	All OSNs
GtαSox2	1:150 FITC-TSA	Sus, multipotent GBCs, HBCs
RbαSox2	1:300 FITC-TSA	Sus, multipotent GBCs, HBCs
MαTuj1	1:800 2°	Immature neurons
GtαCD54	1:50 3°	HBCs
ChkαGFP	1:300 2°	GFP+
RbαGFP	1:200 2°	GFP+
GtαOMP	1:50 2°	Mature neurons
RbαSox9	1:250 2°	Duct/Gland
RbαTRPM5	1:400 FITC TSA	Microvillar
RbαCK18	1:150 2°	Sus
RbαCK18	1:150 2°	Sus
MαPax6	1:100 FITC TSA	Sus, duct/gland, multipotent GBC/HBCs
RbαAq5	1:200 2°	Duct/Gland, HBCs
RbαER	1:300 FITC TSA	CreER+ Cells
GtαNeuroD1	1:200 FITC TSA	Neuronally specified GBCs

Table S2. qRT-PCR Primers Table, Related to STAR Methods

qPCR Primer Name	**Sequence**
NeuroD1 F	GACGGGGTCCCAAAAAGAAAA
NeuroD1 R	GCCAAGCGCAGTGTCTCTATT
Pax6 F	GCGCAGACGGCATGTATGATA
Pax6 R	GGGTTGCCCTGGTACTGAAG
NanogF	TCTTCCTGGTCCCCACAGTTT
NanogR	GCAAGAATAGTTCTCGGGATGAA
OCT4F	GGCTTCAGACTTCGCCTCC
OCT4R	AACCTGAGGTCCACAGTATGC
KLF4F	GTGCCCCGACTAACCGTTG
KLF4R	GTCGTTGAACTCCTCGGTCT
cMYCF	ATGCCCCTCAACGTGAACTTC
cMYCR	CGCAACATAGGATGGAGAGCA
Neurog1 F	GCGCTTCGCCTACAACTACAT
Neurog1 R	CGAGGGACTACTGGGGTCAG
Ascl1 F	GCAACCGGGTCAAGTTGGT
Ascl1 R	GTCGTTGGAGTAGTTGGGGG

Table S3. Table of gRNA Sequences, Related to STAR Methods

gRNA Sequence	Quality Score	Offtargets	Genic offtargets
GTCGTAGGATCCCTCGTCGGAGG	99	9	2
CGACAGGACGCCCGCCTGAAAGG	95	29	8
TCGTCCTACTCCTCCGACGAGGG	93	29	12
CGCCATAGAGTTCAAGTCGTTGG	93	28	2
AACGACTTGAACTCTATGGCGGG	83	61	7
AGCTGCTGGACTTTACCAACTGG	74	209	29